**Design and Testing of a Novel Wide Range – Segmented Gamma Scanner Incorporating Tomographic Gamma Scanning for Measuring both Low and Intermediate Level Waste in Drums-13470**

John A. Mason*, Marc R. Looman*, Lawrence V. Odell*, Adam J. Poundall*, Antony C. N. Towner*, Dae-Seok Hong**, Won-Hyuk Jang**, Kyung-Kil Kwak**, Seung-Min Seo*** and Matt Piotrowski****

*ANTECH, A. N. Technology Ltd., Unit 6, Thames Park, Wallingford, Oxfordshire, OX10 9TA, UK.
**Korea Atomic Energy Research Institute, 111, Daedoek-daero 989 beon-gil, Yuseong-gu, Daejeon, Korea.
***Young In Scientific Co. Ltd, 22, Apgujeong-ro 28 gil, Gangnam-gu, Seoul, Korea.
****ANTECH Corporation, 9050 Marshall Court, Westminster, CO, 80031, USA

**ABSTRACT**
This paper describes the design and testing of a novel automated Wide Range Segmented Gamma ray Scanning (WR-SGS) assay instrument that also incorporates Tomographic Gamma Scanning (TGS).  The instrument is designed for the measurement of both Low and Intermediate Level Waste (LLW and ILW) in 200 litre drums and other waste containers covering a wide range of density.   Like earlier ANTECH WR-SGS instruments, the system employs a single shielded and collimated high purity germanium (HPGe) detector to quantify the radionuclide content of the waste and like conventional SGS instruments it is suitable for the measurement of relatively homogeneous waste matrices. Also, like earlier WR-SGS systems the instrument incorporates an automated variable aperture collimator, which allows the vertical segment height to be adjusted in order to measure both high dose-rate and very low activity drums. The instrument employs both conventional discrete SGS vertical segment measurements as well as vertical segment measurement by continuous helical-scanning of the drum as it rotates. This latter method reduces measurement times for SGS measurements.  In order to determine the density corrections for both low and high-density drums, a high activity Eu-152 transmission source is employed.  When not in use, and in place of a conventional shutter mechanism, the shielded transmission source is moved to a shielded storage position to eliminate background radiation from the source.  Due to its novel features, the WR-SGS is applicable to the measurement of both very low and very high activity waste drums as well as waste drums with a wide range of density.   If located in a low background position and with the effective shielding of the strong transmission source, the instrument can be used to measure very low level or exempt waste.  In order to extend the range of applicability to the measurement of heterogeneous drums, TGS measurement capability has been included in the basic WR-SGS design.   This is achieved by adding horizontal motion to the waste drum rotation platform and incorporating TGS collimation into the variable aperture collimator, as well as a filter to reduce the detector signal when straight-through measurements are made using the strong transmission source.  Test measurements are presented of the system operating in both SGS and TGS modes using different drum densities and source strengths. The test measurement results are compared with benchmarked MCNP Monte Carlo calculations. The Wide Range SGS – TGS instrument extends the range of both activity and density that can be measured in 200 and 340 litre drums.

**INTRODUCTION**

The Wide Range Segmented Gamma Scanner (WR-SGS) has been developed by ANTECH in response to the requirement for a drum waste assay system that is applicable to a wide range of measurement requirements.    These include the ability to measure drums with both low and high activity, low and high-density and in the present case homogeneous and inhomogeneous matrices.    An earlier version of the WR-SGS was developed to satisfy the first two requirements [1, 2].  Operation of the SGS is also based on the original development work performed at the Los Alamos National Laboratory by Martin, Jones and Parker [3].

The instrument described in the present paper represents a further extension of this technology to include Tomographic Gamma Scanning (TGS) capability [4] for measuring drums with inhomogeneous matrices.  Additional features including an automated filter and automation of the detector – drum separation in order to extend the high dose-rate measurement capability of the instrument.   The unit is also designed to handle and measure drums of different sizes from 200 litres (55 US gallons) to 340 litres (85 US gallon over pack).  Figure 1 is an engineering drawing of the instrument showing the input and output roller conveyors and the location of the instrument rack.  Finally the instrument, which has been designated the ANTECH model G3250-3850-340, incorporates additional drum handling features to accommodate drums which are loaded and unloaded on conveyors that arrive at right angles to the drum axis of motion.
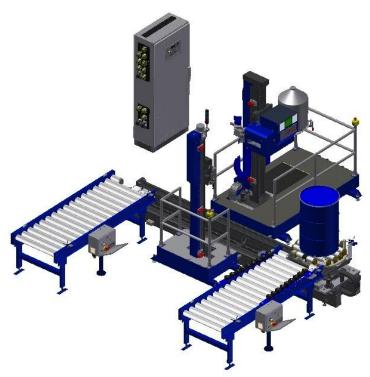


Figure 1.      Engineering drawing of the WR-SGS-TGS showing the location of the control instrumentation rack and the position of the input (right side) and output (left side) drum roller conveyors.

Preliminary performance data is presented based on the use of point sources during commissioning and factory testing. The results have been modeled using the MCNP Monte Carlo Code [5]. The modeling has also been used to generate conversion factors from a point source to a distributed source to assist in the interpretation of the SGS measurement results.

## DESIGN FEATURES OF THE WIDE RANGE SGS WITH TGS

### Variable Aperture Collimator

The Variable Aperture Collimator (VAC) has been described in detail elsewhere [1, 2]. The VAC has been re-designed as part of the present project to reduce manufacturing costs and to incorporate TGS measurement capability. Figure 2 is a three dimensional diagrammatic representation of the VAC showing the HPGe detector lead shield to the rear. The VAC consists of two horizontal tungsten plates, which move closer together or further apart under motor control to change the size of the aperture opening. On either side of the horizontal tungsten plates (which move) are fixed tungsten plates in a "V shaped" orientation creating the SGS collimator.
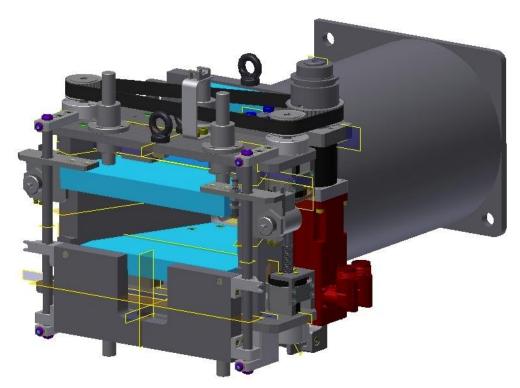


Figure 2. Engineering drawing of the redesigned Variable Aperture Collimator (VAC). Note that the HPGe detector lead shield is shown to the right of the drawing.

Typically, three VAC openings are employed in routine operation: 70 mm, 14 mm and 3.5 mm, corresponding to 100%, 20% and 5% of full opening. A separate calibration is required for each VAC aperture setting or opening. A feature of this technology is that it is possible to use different VAC aperture settings for transmission and emission

measurements. For example, a low-density drum can be measured with a strong transmission source using the 3.5 mm aperture and the emission measurement, where the drum activity is low, can be made with the 70 mm aperture. Alternatively, for very active drums, both transmission and emission measurements can be made with a smaller aperture. The ability to employ different aperture openings for different measurements extends the range of drum density and drum activity to which the instrument is applicable. Although for SGS measurements the instrument is normally operated in two-pass mode (separate transmission and emission measurements) it can also operate in one-pass mode (with a single combined transmission and emission measurement, where appropriate). In this case a single VAC opening is used for both transmission and emission data acquisition during a single scan.
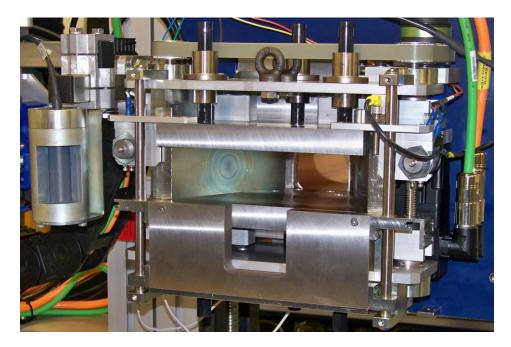


Figure 3.      Photograph of the updated Variable Aperture Collimator (VAC).    Note that the TGS front aperture plate can be seen in the "storage position" below the SGS aperture, which is in the 70 mm 100% open position.   To the left of the SGS aperture is the shielded Geiger Muller dose-rate detector, which is used during the pre-scan measurement.

**Pre-Scanning - Geiger Muller Dose-Rate Detector and Weigh Scale**

Prior to the SGS or TGS measurement, the drum density is determined using the weigh scale (load cell), which is incorporated into the drum rotation mechanism.  The overall drum activity is determined using the dose-rate probe during a pre-scan measurement of the drum. This pre-scan information is then used to choose appropriate VAC apertures for the transmission and emission measurements, as well as the detector distance from the drum and whether or not to deploy the filter (which is described below).  The shielded Geiger Muller dose-rate probe can be seen to the left in Figure 3, where it is mounted on the HPGe detector platform next to the VAC.

**Shielded Transmission Source Safe**

It is necessary to eliminate background radiation arising from the transmission source in order to make low activity measurements with the lowest possible background.  This is often a problem with SGS measurements where, as in the present case, a strong transmission source (740 MBq or 20 mCi of Eu-152) is required to measure drums of higher density.   Even with the use of a conventional shutter mechanism a strong transmission source will still make a significant contribution to the radiation background with the shutter closed.   In order to overcome this problem on the present instrument and the earlier ANTECH WR-SGS instruments, when the source is not in use it is removed to a lead and tungsten shielded storage position.   Using MCNP calculations, the source safe has been designed in such a way that the HPGe detector does not detect any 1408 keV gamma rays from the Eu-152 transmission source.   As a result of this feature, the WR-SGS, if located in a low radiation background area, can be used to measure very low activity drums and samples.   Minimum Detectable Activities (MDA), as a function of density for an equivalent SGS instrument, were reported earlier [1].



Figure 4.  Tungsten shielded transmission source descending into the transmission source safe.

**Helical Scanning for SGS**

For SGS measurements the instrument can operate in conventional fixed-segment mode or in helical scanning mode for both emission and transmission measurements. In helical scanning mode the segment size is determined by a combination of the VAC aperture, the speed of scanning, and the data acquisition or data grab time for each spectrum measurement. As with conventional SGS operation, each segment must correspond to a number of complete drum revolutions; typically this is two, four or more revolutions per helical scanned segment, although the number of revolutions per segment is an adjustable parameter. The helical scanning process produces results, which are entirely equivalent to those obtained from fixed-segment mode scanning. It does, however, have the advantage of a reduced measurement time as data is acquired while the detector is in motion. For

successful helical scanning attention must be paid to ensure that micro-phonic noise in the detector is minimised.  Note that helical scanning is not used in TGS mode.

**Automated Filter**

A motorized tungsten filter of thickness 1 cm has been included immediately to the rear of the VAC and in front of the front face of the HPGe detector.  The operator can control its use or it can be automatically deployed as a result of the dose-rate information obtained during the pre-scam of the drum.

**Automated Detector Positioning**

Earlier WR-SGS instruments permitted the manual horizontal movement of the detector platform so that the separation between the detector and the surface of the drum could be adjusted.   This feature was useful to reduce the dose-rate experienced by the detector and hence the detector dead time.   The movement has been automated with a motor in the present instrument.   The operator can adjust the position of the detector or it can be automatically set as a result of the dose-rate information obtained during the pre-scan of the drum.  A total range of movement of 600 mm is available.   In the present instrument a total of three separate features are available to reduce the dose-rate seen by the detector and allow the instrument to measure very high activity drums.   The features include the VAC, the automated filter and finally the adjustable detector – drum separation.

**Multiple Drum Sizes and Fully Automated Drum Loading/Unloading**

The WR-SGS-TGS is also designed to handle and measure drums of different sizes from 200 litres (55 US gallons) to 340 litres (85 US gallon over pack).  Drum guides on the input conveyor are positioned manually to center drums of the different sizes before they are transferred automatically on to the drum rotation platform, which moves the drums to and from the measurement position.   These guides can be seen in Figure 5 on the right hand end of the input conveyor in the foreground.

Advanced drum handling has been included in the model G3250-3850-340 Wide Range SGS-TGS.   The system incorporates automated input and output roller conveyors, which can be loaded manually (for example with a drum lifter) or automatically by means of other automated conveyors. The drum rotation platform, which incorporates parasitically driven rollers, moves on a slide system between the input and output conveyors and through the drum measurement position.   It also incorporates an internal slide mechanism so the when in the appropriate positions, it can couple to and be parasitically driven by either the input roller conveyor or the output roller conveyor. The drum rotation platform rotates the drums during SGS measurements and both rotates (through 2.5 revolutions) and translates the drums (through a drum radius) during TGS measurements.

**Tomographic Gamma Scanning (TGS)**

Typically most waste drums requiring measurement and assay have matrices that are relatively homogeneous and the measurement errors that arise from SGS measurements fall within acceptable limits. Unfortunately, drums with significant matrix inhomogeneity of either density (absorber) distribution or activity distribution cannot be accurately measured by the SGS method, as very large errors will arise. The TGS capability has been incorporated into the WR-SGS in order to measure the small population of drums with significantly inhomogeneous matrices.

The TGS measurement method has been described in detail elsewhere [4]. TGS measurements are always made in two-pass mode. TGS has lower sensitivity and takes longer than SGS measurements. It has the advantage that maps or images are generated of both the drum density (absorber) distribution and activity distribution. In order to implement TGS measurements, three additional components need to be added to the WR-SGS. These include simultaneous drum rotation and horizontal translation, TGS detector collimation and finally the appropriate TGS analysis software. The TGS collimator is implemented as a movable TGS tungsten front aperture plate, which can be deployed without the use of a separate motor and retained in position for the TGS measurement using shot bolts. The TGS has a fixed size aperture resulting in a fixed segment height of 70 mm. The TGS front aperture plate can be seen (not deployed) in Figure 3.



Figure 5. This is a photograph of the model G3250-3850-340 Wide Range SGS-TGS taken part way through a measurement during the FAT. Note that a drum is in the measurement position on the drum rotation platform. The transmission source is deployed and can be seen immediately to the left of the drum just above the mid-height. Another drum (from the previous measurement) is located on the output roller conveyor. The drum centering guides can be seen on the input roller conveyor in the foreground.

**MONTE CARLO SIMULATIONS**

As with an earlier WR-SGS instruments [1], this instrument has been calibrated and its performance assessed using point sources. In reality, Segmented Gamma Scanners are designed to measure distributed sources. In order to validate the use of point sources for calibration and testing, the point source measurements have been simulated using the MCNP code [5]. This process involves simulating not only the geometry and position of the point sources but also the collimator shield and the detector crystal. The experimental and simulated efficiency data is obtained and generated by dividing the measured net peak area of the gamma ray peak by the number of photons emitted per second for each peak. Four calibration and test drums have been constructed with re-entrant tubes for source location. The drums contain void, sawdust (nominal density 0.169), gel - a polyacrylamide compound with water (nominal density 1.042) and sand (nominal density 1.532).

In order to confirm that the simulated data is correct a comparison between measured and simulated data for point source detection efficiency measurements is presented in Table 1. Although the efficiency data in Table 1 was obtained during SGS scans, the data has not been analysed using the SGS algorithms. That is because these algorithms assume that the source is distributed and these point sources violate that assumption. The data has been analysed as a far field measurement of the point sources. The simulated data models this far field measurement geometry for point sources.

Table I. The table presents the measured and simulated average detection efficiencies for point source measurements performed in three different matrix drums containing sawdust, a gel and sand, each with re-entrant tubes for source deployment. The point source with source Reference Activity, $A_{ref}$, is placed at mid-height of the layer of interest in one of the 3-matrix drums and at the indicated radial position (0, $^2/_3$R and R). The tabulated errors are all for 2 sigma uncertainty [6]. The ratio between the simulated and experimental efficiencies is presented. A significant contribution to the measurement uncertainty is the 3% source calibration error. The symbol $w_E$ designates the collimator opening used during the emission scan.

| ID | Matrix | $w_E$ (mm) | Source | | | Simulated Efficiency $\varepsilon_{Sim}$ | | Experimental Efficiency $\varepsilon_{Exp}$ | | $\varepsilon_{Sim}/\varepsilon_{Exp}$ | |
| | | | Nuc. | Ref. Activity $A_{ref}$ (Bq) | Pos. | Value | Error | Value | Error | Val. | Err. |
|---|---|---|---|---|---|---|---|---|---|---|---|
| 5234567 | Sawdust | 70 | Cs-137 | 7.86E+05 | 0 | 2.10E-05 | 5.26E-09 | 2.05E-05 | 6.37E-07 | 1.02 | 0.03 |
| 6234567 | Sawdust | 70 | Eu-152 | 7.67E+05 | $^2/_3$R | 1.44E-05 | 4.36E-09 | 1.32E-05 | 4.03E-07 | 1.09 | 0.03 |
| 7234567 | Sawdust | 70 | Cs-137 | 7.86E+05 | R | 2.17E-05 | 5.31E-09 | 2.09E-05 | 6.44E-07 | 1.04 | 0.03 |
| 2234567 | Sawdust | 14 | Co-60 | 3.53E+07 | 0 | 1.33E-06 | 1.34E-09 | 1.30E-06 | 3.92E-08 | 1.02 | 0.03 |
| 8234567 | Gel | 70 | Cs-137 | 7.86E+05 | $^2/_3$R | 6.46E-06 | 2.92E-09 | 6.39E-06 | 2.10E-07 | 1.01 | 0.03 |
| 9234567 | Gel | 14 | Co-60 | 3.53E+07 | 0 | 3.18E-07 | 6.55E-10 | 3.54E-07 | 1.08E-08 | 0.90 | 0.03 |
| 1334567 | Sand | 70 | Cs-137 | 7.86E+05 | R | 8.94E-06 | 3.39E-09 | 8.35E-06 | 2.70E-07 | 1.07 | 0.03 |

The measured and simulated data is in good agreement, with the exception of measurement No. 3234567, where it is suspected that the drum was under-scanned as a result of too few drum rotations per segment. This effect was not captured in the MCNP modelling. The data in Table I validates the use of MCNP modelling to simulate drum measurements.

MCNP has also been employed to simulate the detector efficiency for drum scanning in a variety of test drums (matrices), point source positions and collimator aperture openings as shown in Figures 6 and 7.



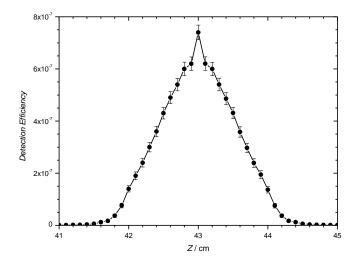Figure 6.      Simulation of the scanning of the sand matrix drum with Co-60 source at the center, and 3.5 mm collimator aperture, 8 segments, segment height 101.25 mm, 8 drum rotations per segment.
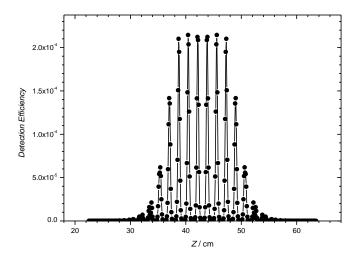


Figure 7.      Simulation of the scanning of the sand matrix drum with Cs-137 source at the drum radius, and 70 mm collimator aperture, 8 segments, segment height 101.25 mm, 6 drum rotations per segment.

Figure 6 displays the detection efficiency result of an MCNP simulation of the central part of the scan of a sand drum with a Co-60 source placed at the center at a height of 43 cm. The scan uses 8 segments, each with a size of 10.1 cm. For a source at the center (or the more realistic case of a distributed source) the number of rotations of the drum is not as important as it would be for a source on the periphery of the drum. Figure 7 is a similar plot for a Cs-137 point source placed at the periphery of a sand filled drum. It is interesting to note that when the source is on the opposite side of the drum to the detector the signal drops to zero. The collimator aperture is 70 mm (fully open).

## SEGMENTED GAMMA SCANNER MEASUREMENTS OF SIMULATED MATRICES

SGS measurements have been performed using Cs-137 and Co-60 point sources placed in drums of different density. These point sources with known and different reference activities, $A_{ref}$, were positioned in one of the three re-entrant source tubes located at the following radial positions: centre (0), two-thirds of radius ($^2/_3$R) or full radius (R) within the three test drums with different density matrices. The results are presented in Table II.

In order to compare point sources measurements with the results of SGS measurements (which assume distributed sources), the apparent activity or "Corrected Activity" of a distributed or volume source that produces the same response in the detector as the point source is calculated. In the table the ratio of the Corrected Activity $A_{cor}$, to the Reference Activity $A_{ref}$ is presented. The values fall within the expected errors, especially when considering that the off centre source positions represent a significant heterogeneity of source distribution. The errors are also larger where the collimator aperture is smaller (14 mm and 3.5 mm) and where the effects of under-scanning and gamma ray contributions through the collimator shielding are more significant.

Table II.        Data is presented from preliminary SGS measurements performed as part of Factory Acceptance Testing of the WR-SGS-TGS with three different matrix drums and Cs-137 and Co-60 point sources. The factor $C_{PV}$ is used to calculate the apparent activity of a volume source resulting in the same detector response as a point source placed at a given radial position. After applying the correction factor the Corrected Activity, $A_{cor}$, is obtained. The Corrected Activity is compared to the Reference Activity.

**Sand ($\rho$ = 1.53 g.cm$^{-3}$)**

| ID | Source | | | Set-up | | Experimental Activity (Bq) | | $C_{PV}$ | $A_{cor}$ (Bq) | $A_{cor}/A_{ref}$ | |
| | Nuc. | Pos. | Ref. Activity $A_{ref}$ (Bq) | P | $w_E$ (mm) | Value | Error | | | Value | Error |
|---|---|---|---|---|---|---|---|---|---|---|---|
| 1274567 | Cs-137 | 0 | 7.86E+05 | F | 70 | 1.66E+05 | 4.13E+03 | 4.59 | 7.63E+05 | 0.97 | 0.05 |
| 1284567 | Cs-137 | 2/3R | 7.86E+05 | F | 70 | 5.79E+05 | 1.18E+04 | 1.28 | 7.43E+05 | 0.94 | 0.05 |
| 1284567Long | Cs-137 | 2/3R | 7.86E+05 | F | 70 | 6.03E+05 | 8.57E+03 | 1.28 | 7.74E+05 | 0.98 | 0.04 |
| 1334567 | Cs-137 | R | 7.86E+05 | F | 70 | 1.11E+06 | 1.32E+04 | 0.62 | 6.86E+05 | 0.87 | 0.04 |
| 1334567_01 | Cs-137 | R | 7.86E+05 | F | 70 | 1.07E+06 | 1.57E+04 | 0.62 | 6.61E+05 | 0.84 | 0.04 |
| 1334567_02 | Cs-137 | R | 7.86E+05 | F | 70 | 1.08E+06 | 1.65E+04 | 0.62 | 6.67E+05 | 0.85 | 0.05 |
| 1334567_03 | Cs-137 | R | 7.86E+05 | F | 70 | 1.11E+06 | 1.64E+04 | 0.62 | 6.86E+05 | 0.87 | 0.04 |
| 1934567 | Cs-137 | R | 7.86E+05 | F | 70 | 1.12E+06 | 1.04E+04 | 0.62 | 6.92E+05 | 0.88 | 0.04 |

**Gel (ρ = 1.02 g.cm⁻³)**

| ID | Source | | | Set-up | | Experimental Activity (Bq) | | $C_{PV}$ | $A_{cor}$ (Bq) | $A_{cor}/A_{ref}$ | |
| | Nuc. | Pos. | Ref. Activity $A_{ref}$ (Bq) | P | $w_E$ (mm) | Value | Error | | | Value | Error |
|---|---|---|---|---|---|---|---|---|---|---|---|
| 1230567 | Co-60 | 0 | 3.22E+04 | F | 70 | 1.58E+04 | 1.18E+03 | 1.70 | 2.69E+04 | 0.83 | 0.09 |
| 1230567long | Co-60 | 0 | 3.22E+04 | F | 70 | 1.61E+04 | 6.80E+02 | 1.70 | 2.74E+04 | 0.85 | 0.06 |
| 9234567 | Co-60 | 0 | 3.53E+07 | F | 14 | 1.85E+07 | 1.14E+05 | 1.71 | 3.16E+07 | 0.90 | 0.07 |
| 1234527 | Co-60 | 0 | 3.53E+07 | B | 14 | 1.96E+07 | 1.76E+05 | 1.84 | 3.62E+07 | 1.02 | 0.13 |
| 1234517_01 | Co-60 | 2/3R | 3.53E+07 | B | 14 | 3.06E+07 | 1.98E+05 | 1.12 | 3.42E+07 | 0.97 | 0.13 |
| 1234517_02 | Co-60 | 2/3R | 3.53E+07 | B | 14 | 3.06E+07 | 1.94E+05 | 1.12 | 3.42E+07 | 0.97 | 0.13 |
| 1234517_03 | Co-60 | 2/3R | 3.53E+07 | B | 14 | 3.01E+07 | 1.93E+05 | 1.12 | 3.37E+07 | 0.95 | 0.13 |
| 1234507 | Co-60 | R | 3.53E+07 | B | 14 | 3.88E+07 | 2.37E+05 | 0.80 | 3.12E+07 | 0.88 | 0.13 |
| 1233567_01 | Cs-137 | 0 | 7.86E+05 | F | 70 | 2.97E+05 | 3.33E+03 | 2.55 | 7.56E+05 | 0.96 | 0.04 |
| 1233567_02 | Cs-137 | 0 | 7.86E+05 | F | 70 | 3.01E+05 | 3.25E+03 | 2.55 | 7.66E+05 | 0.97 | 0.04 |
| 8234567 | Cs-137 | 2/3R | 7.86E+05 | F | 70 | 6.37E+05 | 8.68E+03 | 1.09 | 6.93E+05 | 0.88 | 0.04 |
| 1235567 | Cs-137 | R | 7.86E+05 | F | 70 | 1.07E+06 | 1.11E+04 | 0.70 | 7.46E+05 | 0.95 | 0.04 |

**Sawdust (ρ = 0.17 g.cm⁻³)**

| ID | Source | | | Set-up | | Experimental Activity (Bq) | | $C_{PV}$ | $A_{cor}$ (Bq) | $A_{cor}/A_{ref}$ | |
| | Nuc. | Pos. | Ref. Activity $A_{ref}$ (Bq) | P | $w_E$ (mm) | Value | Error | | | Value | Error |
|---|---|---|---|---|---|---|---|---|---|---|---|
| 1238567 | Co-60 | 0 | 3.22E+04 | F | 70 | 3.45E+04 | 1.21E+03 | 1.03 | 3.57E+04 | 1.11 | 0.05 |
| 1234367_01 | Co-60 | 2/3R | 3.22E+04 | F | 70 | 2.98E+04 | 8.70E+02 | 1.02 | 3.03E+04 | 0.94 | 0.05 |
| 1234367_02 | Co-60 | 2/3R | 3.22E+04 | F | 70 | 2.81E+04 | 8.37E+02 | 1.02 | 2.86E+04 | 0.89 | 0.05 |
| 1234367_03 | Co-60 | 2/3R | 3.22E+04 | F | 70 | 2.95E+04 | 8.53E+02 | 1.02 | 3.00E+04 | 0.93 | 0.05 |
| 1234367_04 | Co-60 | 2/3R | 3.22E+04 | F | 70 | 2.84E+04 | 8.36E+02 | 1.02 | 2.89E+04 | 0.90 | 0.05 |
| 1234867_01 | Co-60 | 2/3R | 3.53E+07 | B | 14 | 3.12E+07 | 1.29E+05 | 1.06 | 3.32E+07 | 0.94 | 0.03 |
| 1234867_02 | Co-60 | 2/3R | 3.53E+07 | B | 14 | 3.09E+07 | 1.27E+05 | 1.06 | 3.29E+07 | 0.93 | 0.03 |
| 1237567 | Co-60 | R | 3.22E+04 | F | 70 | 2.78E+04 | 8.15E+02 | 1.02 | 2.84E+04 | 0.88 | 0.05 |
| 1234167_01 | Co-60 | R | 3.22E+04 | F | 70 | 2.97E+04 | 8.72E+02 | 1.02 | 3.03E+04 | 0.94 | 0.05 |
| 1234167_02 | Co-60 | R | 3.22E+04 | F | 70 | 2.97E+04 | 8.55E+02 | 1.02 | 3.03E+04 | 0.94 | 0.05 |
| 1234167_03 | Co-60 | R | 3.22E+04 | F | 70 | 3.03E+04 | 8.58E+02 | 1.02 | 3.09E+04 | 0.96 | 0.05 |
| 1234167_04 | Co-60 | R | 3.22E+04 | F | 70 | 3.57E+04 | 1.01E+03 | 1.02 | 3.65E+04 | 1.13 | 0.05 |
| 1234167_05 | Co-60 | R | 3.22E+04 | F | 70 | 3.08E+04 | 8.73E+02 | 1.02 | 3.15E+04 | 0.98 | 0.05 |
| 1234167_06 | Co-60 | R | 3.22E+04 | F | 70 | 3.00E+04 | 8.64E+02 | 1.02 | 3.06E+04 | 0.95 | 0.05 |
| 1234967_01 | Co-60 | R | 3.53E+07 | B | 14 | 3.18E+07 | 1.28E+05 | 1.04 | 3.31E+07 | 0.94 | 0.03 |
| 1234967_02 | Co-60 | R | 3.53E+07 | B | 14 | 3.20E+07 | 1.29E+05 | 1.04 | 3.33E+07 | 0.94 | 0.03 |
| 5234567 | Cs-137 | 0 | 7.86E+05 | F | 70 | 7.29E+05 | 5.52E+03 | 1.08 | 7.85E+05 | 1.00 | 0.03 |
| 5234567 | Cs-137 | 0 | 4.01E+06 | F | 70 | 3.83E+06 | 2.64E+04 | 1.08 | 4.12E+06 | 1.03 | 0.03 |
| 1236567 | Cs-137 | 2/3R | 7.86E+05 | F | 70 | 7.97E+05 | 4.75E+03 | 1.10 | 8.79E+05 | 1.12 | 0.03 |
| 1234767 | Cs-137 | 2/3R | 7.86E+05 | B | 14 | 7.44E+05 | 2.51E+04 | 1.06 | 7.87E+05 | 1.00 | 0.05 |
| 1234467_01 | Cs-137 | 2/3R | 4.01E+06 | B | 14 | 3.75E+06 | 5.68E+04 | 1.06 | 3.97E+06 | 0.99 | 0.03 |
| 1234467_02 | Cs-137 | 2/3R | 4.01E+06 | B | 14 | 3.79E+06 | 5.73E+04 | 1.06 | 4.01E+06 | 1.00 | 0.03 |
| 7234567 | Cs-137 | R | 7.86E+05 | F | 70 | 8.42E+05 | 5.91E+03 | 1.04 | 8.76E+05 | 1.11 | 0.03 |
| 1834567H | Cs-137 | R | 7.86E+05 | F | 14 | 6.73E+05 | 1.55E+04 | 1.02 | 6.84E+05 | 0.87 | 0.05 |
| 1234667_01 | Cs-137 | R | 4.01E+06 | B | 14 | 4.05E+06 | 5.99E+04 | 1.02 | 4.14E+06 | 1.03 | 0.03 |
| 1234667_02 | Cs-137 | R | 4.01E+06 | B | 14 | 4.67E+06 | 6.82E+04 | 1.02 | 4.78E+06 | 1.19 | 0.03 |
| 6234567 | Eu-152 | 2/3R | 7.67E+05 | F | 70 | 7.13E+05 | 4.47E+03 | 1.01 | 7.19E+05 | 0.94 | 0.04 |
| 6234567 | Eu-152 | 2/3R | 7.67E+05 | F | 70 | 6.98E+05 | 6.92E+03 | 1.01 | 7.04E+05 | 0.92 | 0.04 |
| 6234567 | Eu-152 | 2/3R | 7.67E+05 | F | 70 | 6.89E+05 | 6.82E+03 | 1.01 | 6.95E+05 | 0.91 | 0.04 |
| 6234567 | Eu-152 | 2/3R | 7.67E+05 | F | 70 | 7.00E+05 | 4.42E+03 | 1.01 | 7.06E+05 | 0.92 | 0.04 |

## TOMOGRAPHIC GAMMA SCANNER MEASUREMENTS OF SIMULATED MATRICES

The results of preliminary TGS measurements using the WR-SGS-TGS are displayed in Figure 8 and tabulated in Table III. Figure 8 displays the results of three TGS measurements, one with Cs-137 point sources in a gel filled drum and two with the same sources deployed in void drums, the latter one containing an iron absorbing block. The TGS images show the location of both the sources and the distribution of absorber (high density regions). The location of two separate sources can be seen in Figure 8 g).
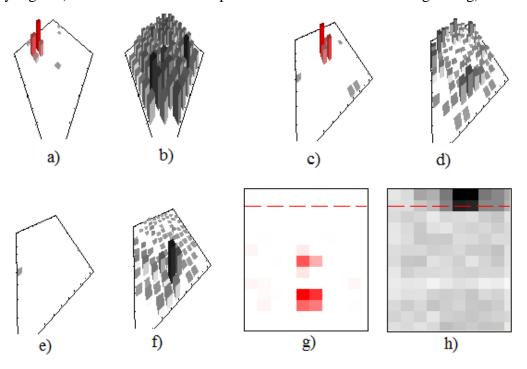


Figure 8.    Figure 8 a) emission and b) transmission - measurement output figures for segment 7 of the TGS measurement of two Cs-137 sources placed in a re-entrant tube in a gel drum. Note the relatively high density of the matrix. Figure 8 c) emission and d) transmission - measurement output figures for segment 7 of the TGS measurement of two Cs-137 sources placed in a re-entrant tube in a void drum. Note the lower matrix density. The peripheral cylindrical region is the steel of the drum. Figure 8 e) emission and f) transmission - measurement output figures for segment 7 of the TGS measurement of two Cs-137 sources placed in a re-entrant tube in a void drum into which a steel block has also been introduced. Figure 8 g) emission and h) transmission - measurement output figures for side views of the whole drum shown in Figure 8 e) and f).  Note that in this latter measurement the two sources are at separate heights in the drum and the position of the steel block absorber can be seen clearly in figure 8 h). The TGS results for the three measurements are tabulated in Table III. In the first two tests two Cs-137 point sources were placed together and appear as one single source where the TGS has correctly determined the total activity. In the third test the sources were separated and placed in different segments. Again for this third test the TGS has correctly determined the total activity.

Table III.      The results of TGS measurements employing two Cs-137 point sources (330 kBq and 790 kBq) placed at different positions inside the re-entrant tubes of test drums containing various matrices.

| ID | Matrix | Net Mass (kg) | Nuclide | Reference Activity $A_{ref}$ (Bq) | Reported Activity $A_{rep}$ (Bq) | $A_{rep}/A_{ref}$ |
|---|---|---|---|---|---|---|
| 1 | Gel | 213 | Cs-137 | 1.120E+06 | 1.193E+06 | 1.065 |
| 2 | Void | 1.6 | Cs-137 | 1.120E+06 | 1.069E+06 | 0.954 |
| 3 | Void + Lead Brick | 7 | Cs-137 | 1.120E+06 | 1.133E+06 | 1.012 |

## CONCLUSIONS

An enhanced performance Wide Range SGS-TGS with a number of novel features has been designed, built and tested. The unit has been calibrated and then tested in both SGS and TGS operating modes using a variety of point sources. SGS performance has been confirmed using MCNP Monte Carlo modeling which incorporates all aspects of the detector, collimator, drum and source geometry. The validity of the MCNP modeling has been confirmed by comparing far field measurements of the point sources in various drum positions with MCNP simulations.

SGS measurements have been performed with point sources located in a variety of positions in three drums with different matrix densities. These measurement results have been compared with simulations assuming distributed sources, which produce an equivalent response in the HPGe detector. In this way the performance of the SGS measurements has been validated. Good agreement (within expected errors) has been achieved for the SGS measurements.

As an alternative to varying the collimator aperture of the VAC, varying the distance of the detector from the drum surface can also reduce detector dead time, and this axis is now automated.  Higher activity drums can be measured using a larger VAC aperture (for example 14 mm) in the rear detector position avoiding the possibility of under-scanning, which can arise when using the 3.5 mm aperture in the detector forward position.  This improved approach has been used in measuring the higher activity Co-60 source in the low-density sawdust matrix.

TGS measurements have also been performed for drums with both void and medium density matrices. Very good quantitative results have been obtained for the measurement of the activity of Cs-137 sources placed in the drums. TGS images have also been obtained showing the correct location of the sources and the correct location of an attenuating block of steel placed in one of the drums.

The automated Wide Range SGS-TGS represents a significant development in the technology for radioactive waste measurement.

**REFERENCES**

1. J. A. Mason, M. R. Looman, R. A. Price, A. C. N. Towner, R. Kvarnström and H. Lampen, "Design and Operation of a Wide Range Segmented Gamma Ray Scanning Assay Instrument for the Measurement of both Low and Intermediate Level Waste", Proceedings of INMM11, Palm Springs, CA, July 2011. (11-A-424-INMM)

2. John A. Mason, Marc R. Looman, Antony C. N. Towner, Kapila Fernando, Roland Wong, Robert A. Price, Bret Taylor and Paul Anderson, "Calibration and Validation of a Wide Range Segmented Gamma ray Scanning Instrument for the Measurement of Low and Intermediate Level Waste", Proceedings of ICEM11, Reims, Champagne Congres, France, September 2011. (ICEM11-59304)

3. E. R. Martin, D. F. Jones, and J. L. Parker, *Gamma Ray Measurements with the Segmented Gamma Scan*, Los Alamos Scientific Laboratory, LA-7059-M, 1977.

4. J. A. Mason, A. C. Tolchard, A. C. N. Towner, K. J. Burke, R. A. Price, S. Dittrich, M. Piotrowski, F. Zurey and D. Walraven, *A Tomographic Segmented Gamma Scanner for the Measurement of Decommissioning Wastes*, Proceedings of ICEM03, Examination School, Oxford, England, September 2003. (ICEM03-4658)

5. J. F. Briesmeister, *MCNP - A General Monte Carlo N-Particle Transport Code (Version 4C)*, Los Alamos National Laboratory, LA–13709–M, 2000.

6. L. A. Currie, *Limits for Qualitative Detection and Quantitative Determination*, Analytical Chemistry, 40 (3), p. 586-593, March 1968.